JOURNAL OF Materials CHEMISTRY

New variants of polymorphism in banana-shaped mesogens with cyano-substituted central core†

Ina Wirth,[a] Siegmar Diele,[a] Alexei Eremin,[a] Gerhard Pelzl,*[a] Siegbert Grande,[b] Laura Kovalenko,[a] Natella Pancenko[a] and Wolfgang Weissflog[a]

[a]*Institut für Physikalische Chemie, Martin-Luther-Universität Halle-Wittenberg, Mühlpforte 1, 06108 Halle/S., Germany. E-mail: pelzl@chemie.uni-halle.de*
[b]*Fakultät für Physik und Geowissenschaften, Universität Leipzig, Linnéstraße 5, 04103 Leipzig, Germany*

Received 26th January 2001, Accepted 30th March 2001
First published as an Advance Article on the web 24th April 2001

A new series of achiral five-ring banana-shaped compounds is presented which exhibit a cyano substituent in the 4-position of the central core. It follows from X-ray investigations and from NMR, microscopical and electro-optical measurements that all members of the series do not only form the chiral B_2 phase characteristic of a bent molecular shape, but also SmA and SmC (in one case also nematic) phases. The electro-optical studies on the B_2 phase prove an antiferroelectric ground state which can be switched into ferroelectric states. On the base of the experimental data plausible structure models have been proposed.

In 1996 it was found by Niori *et al.*[1] that the smectic high-temperature phase of a banana-shaped compound showed ferroelectric switching. Detailed current response measurements on this switchable mesophase gave evidence that the ground state is antiferroelectric.[2–5] The unexpected antiferroelectric properties of this mesophase preliminarily designated as the B_2 phase stimulated the synthesis of new materials with a bent molecular shape (ref. 6 and references therein). Up to now four additional smectic-like mesophases without in-plane order could be distinguished which are designated as B_1, B_5, B_6 and B_7, where two of them (B_5, B_7) exhibit antiferroelectric switching behaviour, too.[6]

Recently we described an achiral bent five-ring mesogen which possesses a cyano group in the 4-position of the central core.[7] It was shown by X-ray diffraction measurements and electro-optical investigations that this compound not only exhibits a B_2 phase specific for a bent molecular shape but in addition a SmA and a SmC phase characteristic for calamitic liquid crystals.

In this paper we present 5 further homologous banana-shaped compounds with a cyano-substituted central core. For all compounds studied we found a B_2 phase as well as a SmA and/or a SmC phase. For the homologue with the shortest terminal chains an additional nematic phase could be observed. On the basis of X-ray and NMR investigations an attempt has been made to propose plausible structure models and to discuss the molecular origin of this unusual phase behaviour.

Materials

The synthetic route is shown in Scheme 1. The elimination of water from 2,4-dihydroxybenzaldoxime prepared from 2,4-dihydroxybenzaldehyde was performed according to a slight modification of the procedure of Serrano *et al.*[8] with acetic anhydride and following deprotection of the acetate to give 2,4-dihydroxybenzonitrile.[9] The esterification with 4-(4-alkyl- or alkyloxy-phenyliminomethyl)benzoic acid[10] was successful by means of DCC–DMAP.

Table 1 presents the phase transition temperatures and the transition enthalpies of the substances studied. In the table the results of phase assignment are anticipated.

Results

Texture observation and electro-optical investigations

Compounds C_{12} and C_{14}. Compound **C_{14}** was the first bent-shaped compound for which a polymorphism B_2–SmC–SmA was reported.[7] The three mesophases could be clearly distinguished on the basis of their characteristic textures and their electro-optical response. As seen from Table 1 the dodecyl homologue **C_{12}** shows a mesomorphic dimorphism B_2–SmA. The SmA phase forms a homeotropic or a fan-shaped texture whereas the B_2 phase exhibits a *schlieren* or a broken (grainy) fan-shaped texture. The B_2 phase could be clearly assigned from the results of electro-optical investigations.

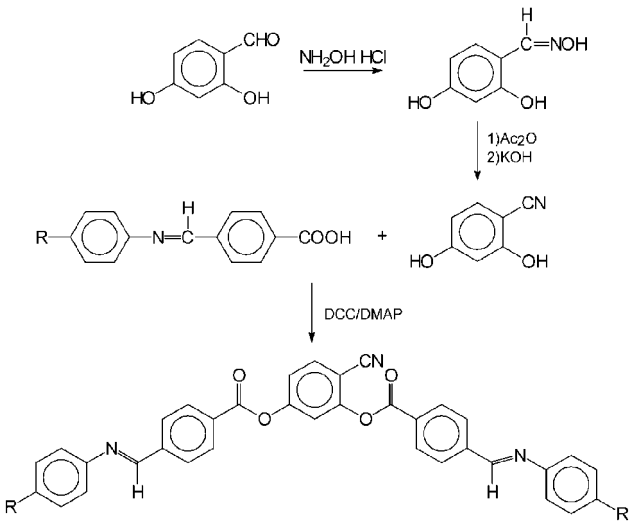

Scheme 1

†Electronic supplementary information (ESI) available: colour versions of Fig. 2, 3, 8 and 10. See http://www.rsc.org/suppdata/jm/b1/b100924i/

 DOI: 10.1039/b100924i

Table 1 Transition temperatures/°C [transition enthalpies/kJ mol^{-1}][a]

Compound	R	Cr	B_2	SmC	SmA	N	I
C_{12}	$C_{12}H_{25}$	• 80 [13.2]	• 124 [1.3]	—	• 164 [6.8]	—	•
C_{14}[7]	$C_{14}H_{29}$	• 90 [19.5]	• 128 [1.8]	• 142 [—]	• 166 [7.6]	—	•
C_6O	OC_6H_{13}	• 122 [32.3]	(• 103) [0.2]	• 133 [1.8]	• 156 [0.6]	• 165 [0.9]	•
C_8O	OC_8H_{17}	• 97 [37.4]	• 142 [1.9]	• 146 [2.1]	• 175 [4.8]	—	•
C_9O	OC_9H_{19}	• 62 [45.9]	• 134 [3.5]	• 138.5 [2.7]	• 180 [5.8]	—	•
$C_{12}O$	$OC_{12}H_{25}$	• 65 [14.7]	• 122 [4.8]	• 141 [—]	• 188 [7.2]	—	•

[a]Cr: crystalline; I: isotropic; SmA, SmC: smectic A or smectic C, respectively; N: nematic; B_2: B_2 mesophase. The numbers between the phase symbols designate the phase transition temperatures in °C, the numbers below which are the transition enthalpies in kJ mol^{-1} (in square brackets). Parentheses indicate monotropic transitions.

The initially "grainy" fan-shaped texture forms a smooth SmA-like fan-shaped texture after the first switching. The switched state depends on the polarity of the applied field indicating an antiferroelectric switching typical for a B_2 phase.

Compounds C_6O, C_8O, C_9O and $C_{12}O$. As seen from Table 1 the homologue with the shortest terminal chain exhibits a polymorphism B_2–SmC–SmA–N. This is the first case in which the B_2 phase and a nematic phase are observed in the same substance. It is remarkable that the phase transition SmC→SmA is first order; the transition enthalpy (1.8 kJ mol^{-1}) is higher than that for the transitions SmA–N (0.6 kJ mol^{-1}) or N–I (0.9 kJ mol^{-1}), whereas the transition enthalpy SmC→B_2 is extremely low (0.2 kJ mol^{-1}). It cannot be excluded that this transition SmC–B_2 is second order. The B_2 phase could be identified by its characteristic electro-optical behaviour. On applying a triangular voltage two current peaks occur per half period (see Fig. 1). It is seen from Fig. 2 that the switched states depend on the sign of the electric field indicating a "homochiral" ground state.[4] From the field-induced change of the extinction direction at crossed polarizers a tilt angle of 15° could be estimated. In the SmC phase only a field-induced change of the interference colour is observed above a threshold voltage which is independent of the polarity of the field and which also occurs in ac fields up to 5 kHz. These findings point to a dielectric reorientation (Freedericksz transition).

The longer-chained homologues **C_8O**, **C_9O** and **$C_{12}O$** form the B_2 phase in the sequence B_2–SmC–SmA (Table 1). In the case of compounds **C_8O** and **C_9O** the transition SmA→SmC is indicated by the change from a homeotropic texture into a dark *schlieren* texture with pronounced fluctuations whereas the fan-shaped texture of SmA does not markedly change. At the transition SmC→B_2 the fan-shaped texture is transformed into a broken and grainy fan-shaped texture whereas the *schlieren* texture of SmC becomes more strongly birefringent and less fluctuating. Both transitions are accompanied by a clear peak in the DSC curve. In the B_2 phase "homochiral" and "racemic" domains are observed.

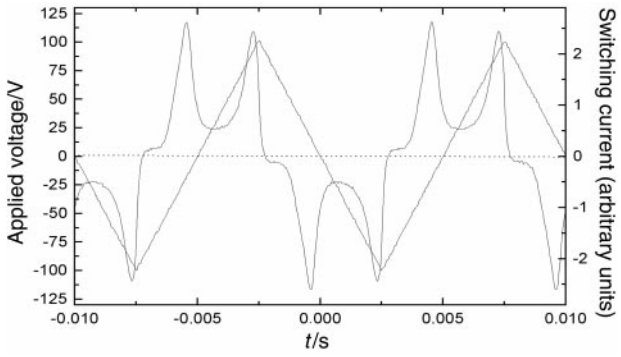

Fig. 1 Switching current response of the B_2 phase of compound **C_6O** at 75 °C by using the triangular wave method (cell thickness: 6 μm; 100 Hz, 100 Vpp (Vpp = volt peak-to-peak)).

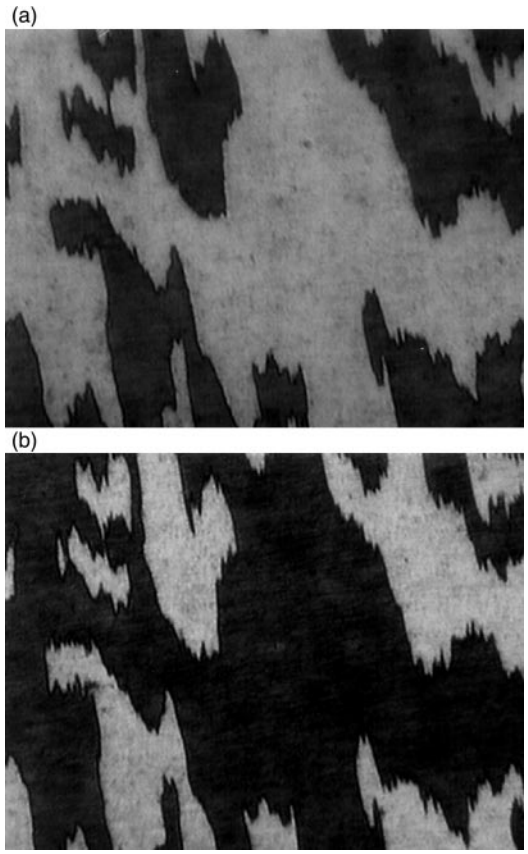

Fig. 2 Optical textures in the B_2 phase of compound **C_6O** and their dependence on the polarity of the applied field: a) −80 V, b) +80 V.

In the "racemic" domains the switched states are independent of the polarity of the applied field. In "homogeneously chiral" domains the texture of the switched states is different for opposite signs of the field. In both cases two current peaks could be recorded per half period of a triangular voltage indicating an antiferroelectric ground state of the B_2 phase. For compound **C_9O** the antiferroelectric switching was observed up to 30 °C. With decreasing temperature the threshold voltage clearly increases probably as a consequence of the higher elastic constants. Furthermore, also the switching times become longer with decreasing temperature obviously due to the increasing viscosity.

In contrast to the B_2 phase, the SmC phase does not show a current response. Similar to compound **C_6O** a less pronounced switching occurs up to a frequency of about 5 kHz which can be explained by a dielectric reorientation. For compound **C_9O** parallel black stripes perpendicular to the initial director direction arise in the planar oriented SmC phase (Fig. 3). The period of these stripes (1.6 μm) is clearly smaller than the cell thickness (6 μm). The domain pattern shows the characteristic feature of the electrohydrodynamic "fundamental" domains which obviously correspond to the dielectric regime of the SmC phase.[11]

In some respects compound **$C_{12}O$** behaves quite similarly to compound **C_{14}** because the transition SmC→B_2 is first order and the transition SmC–SmA is second order. The electro-optical behaviour is similar to that of compound **C_{14}** which could be followed up to 30 °C whereby also large homogeneous domains were obtained.

In order to study the effect of a chiral dopant on the

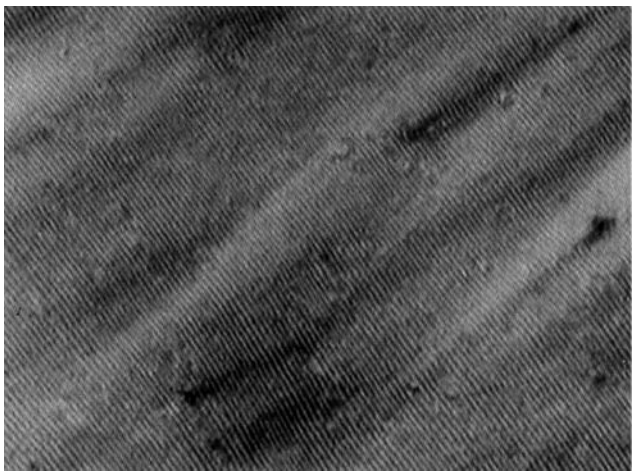

Fig. 3 Electrohydrodynamic domain pattern in the SmC phase of compound **C_9O** (temperature: 136 °C, cell thickness: 6 μm; voltage: 36 V; period of the domains: 1.8 μm; the stripes are perpendicular to the original director direction).

electro-optical behaviour of the B_2 and SmC phase we doped compound **C_{14}** with 1.2 wt% of cholesteryl octanoate which exhibits a cholesteric mesophase [Cr 80.5(SmA 77.5) N* 92 I]. By the addition of the chiral dopant the transition temperatures are only slightly depressed. We found that the switching behaviour of the B_2 phase was not markedly changed by a chiral dopant. We observed the characteristic texture change (Fig. 4d–f) and a current response which corresponds to an antiferroelectric switching. But in contrast to the non-doped compound the greatest part of the sample showed a uniform handedness; that means that the chiral dopant favours one definite handedness.

On the other hand, the electro-optical response of the SmC phase was completely changed by the chiral additive. In the non-doped SmC phase only a weak switching effect independent of the polarity of the field was observed up to relatively high frequencies (~5 kHz). In the sample with a chiral dopant the switching behaviour becomes nearly identical with that of the B_2 phase; as seen from Fig. 4a–c, the same switchable

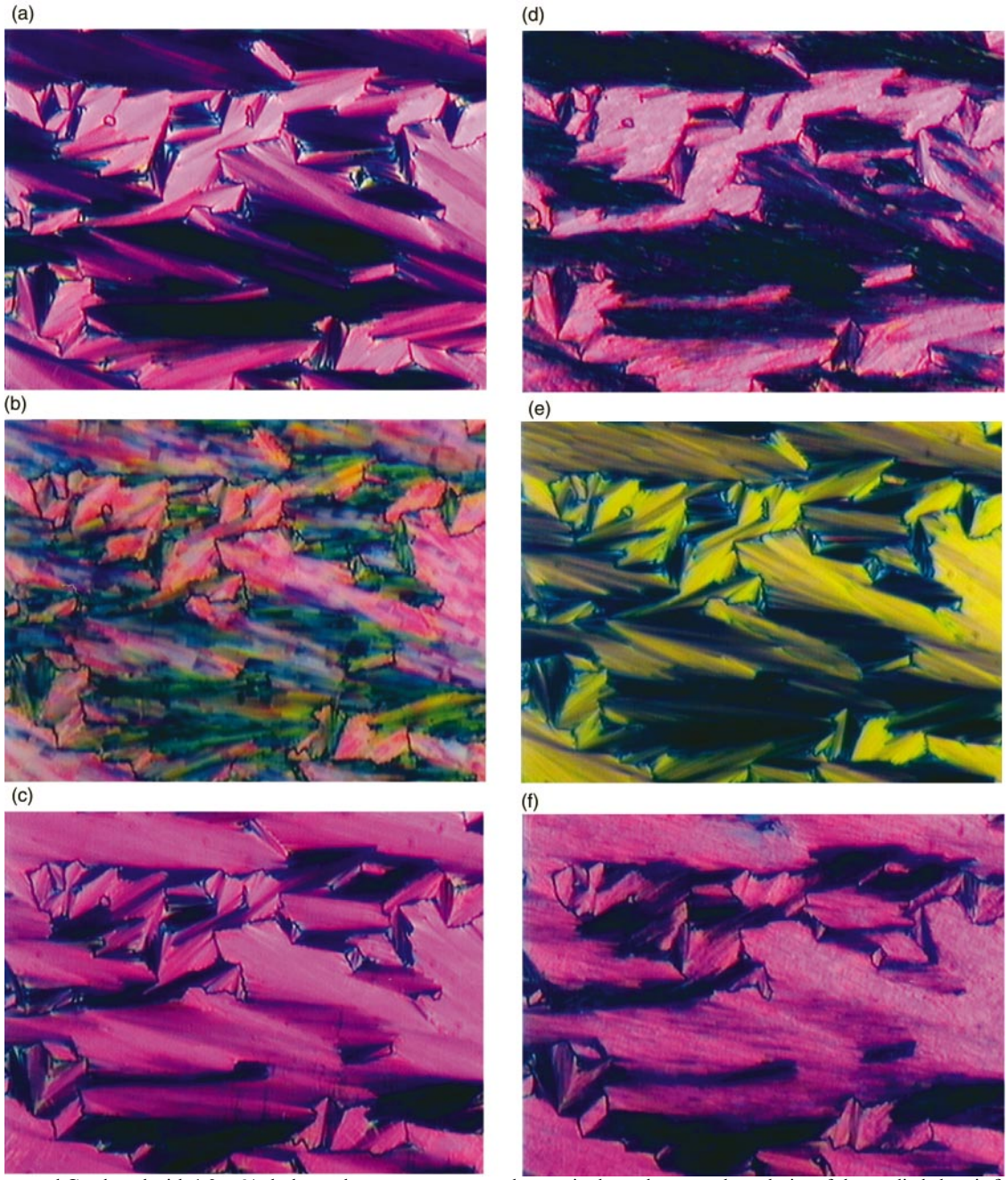

Fig. 4 Compound **C_{14}** doped with 1.2 wt% cholesteryl octanoate: texture changes in dependence on the polarity of the applied electric field (sample thickness 6 μm). SmC (124 °C): a) −6 V, b) 0 V, c) +6 V; B_2 (119 °C): d) −12 V, e) 0 V, f) +12 V.

domains are visible in dependence on the polarity of the field. In contrast to the B_2 phase the threshold is clearly reduced. Unfortunately, we were not able to detect a current response in the SmC phase, probably because the tilt of the molecules and therefore the spontaneous polarization are rather low. These experiments indicate that the SmC phase is obviously transformed into an antiferroelectric SmC_A phase since the switching behaviour is analogous to that of the B_2 phase.

NMR measurements. We investigated two samples, one with a short alkyloxy chain (**C_6O**) and the other with a longer alkyl chain (**C_{14}**). The labelling of the atoms in the molecule is shown in Fig. 5. As seen we designate the rings by A, B, C and the methylene carbons by x_n starting at the outer aromatic ring.

The aromatic part in the isotropic spectra is different for the two materials due to the different substituents at C1. Fig. 6 demonstrates the spectral resolution together with assignment of the lines for **C_6O** in the isotropic and liquid crystalline phase. Nearly all positions in the aromatic regions are resolved also in liquid crystalline phases, however overlapping exists at few temperatures. As seen in Fig. 6 the anisotropic shifts of equivalent positions in the two legs are different. The aliphatic carbons are resolved only for the short chain of **C_6O**. We measured the temperature dependence of the carbon shifts with decreasing temperature.

For the interpretation we neglected the contribution from D, the anisotropic order fluctuations parameter, to the anisotropic shift. All our evidence points to a D no larger than for linear molecules. Therefore the influence of a small D on the interesting geometry data is small and the observed temperature dependence of the ^{13}C chemical shift in the liquid crystalline phases is directly related to the order parameter S:

$$\delta^i_{obs}(T) = \delta^i_{iso} + S\delta^i_{\zeta\zeta}$$

$\delta^i_{\zeta\zeta}$ are the ζ components of the shift tensors of carbon i in the molecular system ξ, η, ζ where ζ corresponds to the molecular long axis. The $\delta^i_{\zeta\zeta}$ depend on the orientation and magnitude of the main frame shift tensors. The central ring C with C9 and C10 has a well defined geometry in the case of symmetric substitution. The ζ axis has a symmetrical position (Fig. 5) and the C–H or C–O bonds form angles of 30° with this axis. The coordinate η is chosen perpendicular to the plane of the ring C.

In the present molecules with nonsymmetric CN-substitution the symmetry is lost; ζ can deviate from the symmetry direction. In addition, the substitution changes the shift tensors for all carbons of ring C in comparison to the values obtained for the symmetric rings.[5,12] The CN line is visible in the spectra at higher temperatures as a broad line, but the observation helps us in the interpretation. The problem is that the measured anisotropic shifts are always the product of geometry ($\delta_{\zeta\zeta}$) and order S and can not be separated.

Reasonable results are obtained for a value of

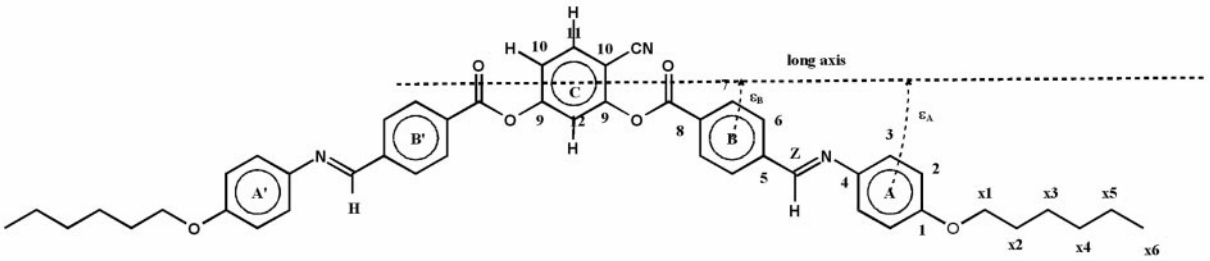

Fig. 5 Sketch of the **C_6O** molecule and assignment of atoms and rings.

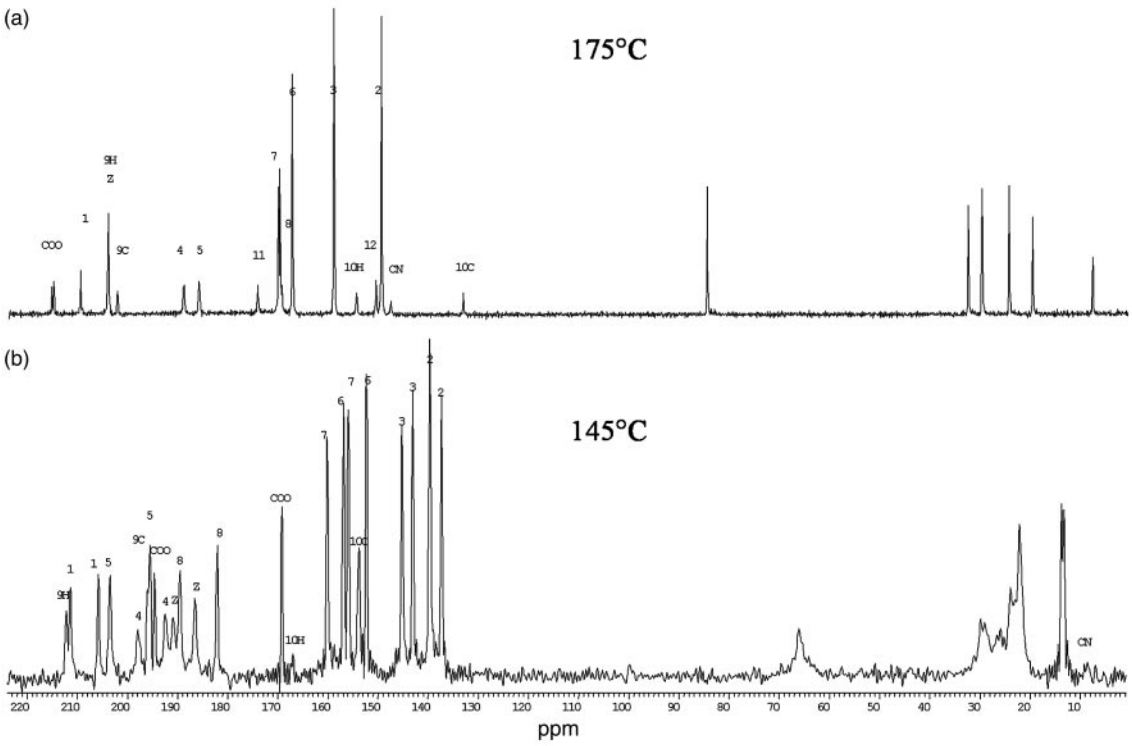

Fig. 6 ^{13}C spectra of the isotropic (a) and B_2 phase (b) of compound **C_6O**.

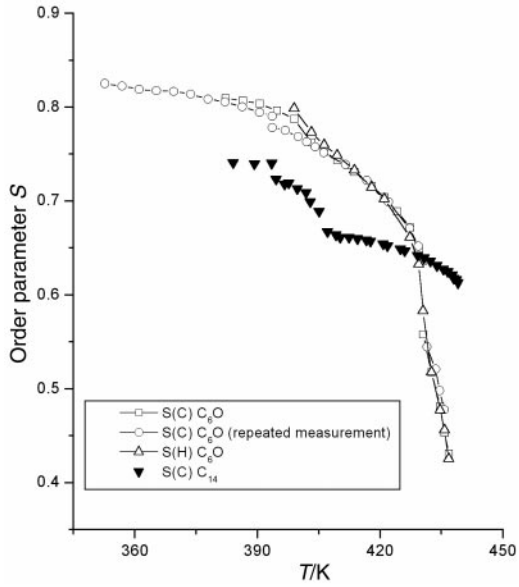

Fig. 7 Temperature dependence of the orientational order parameter in the mesophases of compounds **C_6O** and **C_{14}**. *S*(C): by anisotropic ^{13}C-shift of ring C carbons; *S*(H): by dipolar proton splitting of ring C.

$\delta^{CN}_{\zeta\zeta} = -151$ ppm. The choice is arbitrary but can not vary more than 5% having in mind the obtained order parameter *S* (a variation of this value changes the calculated $\delta^i_{\zeta\zeta}$ by the same factor and therefore all geometrical data). The ratio of the CN shift to the other anisotropic shifts of the carbons in the central ring C gives reasonable $\delta^i_{\zeta\zeta}$ comparable to other similar substituted molecules. Assuming an axial symmetric main frame tensor of −205 ppm for the C(N)[13] we obtain an angle of 25° between the C–CN direction and the long axis (a deviation of 5° from the symmetrical direction). The same values are assumed for both types of molecules. The ratios of the anisotropic shifts are independent of the temperature. This result excludes a change in the direction of the long axis more than 0.5° over the liquid crystalline temperature regions.

The accepted $\delta^i_{\zeta\zeta}$ values for the central ring C now determine the order parameter *S*. The temperature dependence is shown in Fig. 7. *S* varies from 0.42 for the nematic phase to 0.82 for the low temperature phase of **C_6O**. These are typical values for nematic and smectic phases and justify our supposed $\delta^i_{\zeta\zeta}$ of ring C. Repeated measurements of the **C_6O** sample yield a decrease and a broadening of the transition regions, which is visible in the *S*(*T*) curves.

The ^{1}H spectra in the liquid crystalline phase resolve a splitting of broad lines (proton pairs of ring A and B) overlapped by a splitting of sharper lines (H10–H11 pair). The order parameter *S*(H) calculated from this dipolar splitting agrees with that obtained by ^{13}C shift if we assume the same angle of 25° between C–(CN) and the long axis. The *S* values in **C_{14}** at the transition SmC→B_2 and within the B_2 phase are below the values of **C_6O**.

The calculated *S*(*T*) is now used to obtain the $\delta^i_{\zeta\zeta}$ for all carbons in the two legs. The observed time averaged values are connected to the main frame shift tensor (δ_{11}, δ_{22}, δ_{33}) by the relation:

$$\delta^i_{\zeta\zeta} = \delta^i_{11}\cos^2\varepsilon + \left(-\frac{\delta^i_{11}}{2} + \left(\frac{\delta^i_{11}}{2} + \delta^i_{22}\right)\cos(2\phi)\right)\sin^2\varepsilon$$

The exact knowledge of the main frame shift tensor allows the calculation of ε (the angle between the *para*-axis of the corresponding ring and the long axis ζ) and φ (the torsion angle between the ring plane and the ξζ-plane). The different shifts of the two legs are therefore connected with different angles ε and

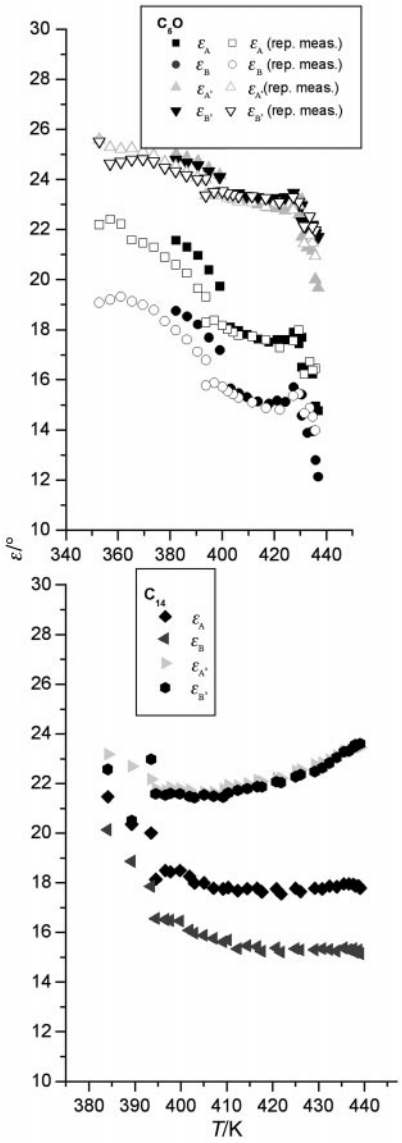

Fig. 8 Angle ε (°) between the long molecular axis and the 4 aromatic rings (A, A′, B, B′) in the mesophases of compounds **C_6O** and **C_{14}** calculated from $\delta_{\zeta\zeta}$ and reference values of two-ring liquid crystalline materials. We assumed axial symmetric tensors of the rings (or torsion angles near 45°).

φ. For δ^i_{11} we used values derived from simple linear liquid crystalline reference compounds with the same substituents and for δ^i_{22} typical values from the literature. The precise knowledge especially of δ^i_{11} has an influence on the geometrical data. It follows from our calculations that the φ values are near 45°. According to the formula above in this case the anisotropy of the shift tensor can be neglected. With this simple approximation we need only δ^i_{11} and we optimized these values to obtain nearly the same angle from the 4 carbons within one ring.

In Fig. 8 the angles ε calculated in this way for the 4 rings A, A′, B, B′ in the two legs are shown for **C_{14}** and **C_6O**. The relative error and the scattering of the data are large in the nematic phase of **C_6O** due to broad lines in the spectra, the same is valid for the B_2 phase of **C_{14}**. The angle ε varies with temperature for all 4 rings. For one leg (our proposal is the right site, where CN is substituted) ε is smaller for the inner ring B (15° in the SmA phase) than for the outer ring A (18° for SmA), which means the bending increases towards the outer part. The values agree for the two materials independent of the chain length. At the transition to the SmC phase the angles increase in **C_6O** evidently for the whole leg (Fig. 8). The change of ε is slower for the second measurement but reaches the same

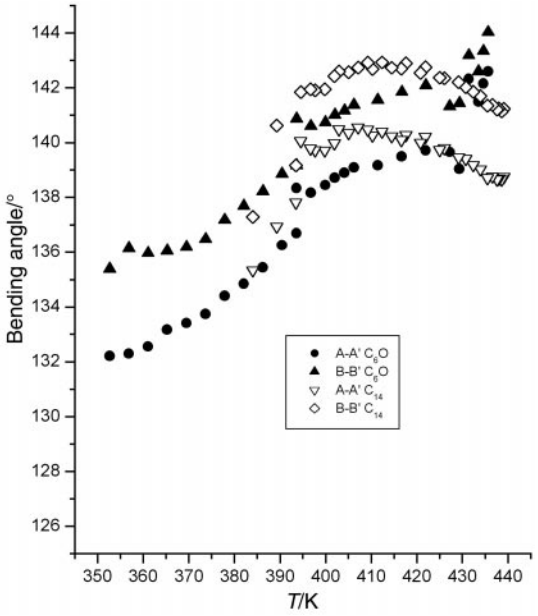

Fig. 9 Bending angle between the two legs of the molecules ($180°-\varepsilon-\varepsilon'$) in the mesophases of compounds **C_6O** and **C_{14}**, respectively.

final values, so it seems that the intermolecular forces support a change in bending. The increase of ε is small in the short region of the SmC phase of **C_{14}**. The behaviour of the other leg differs for the two materials. In **C_6O** both rings have identical angles (23°), nearly constant within the SmA phase and increasing at the transition to the SmC phase. In **C_{14}** the angle ε starts also with values of 23°, but here the angles decrease with decreasing temperature. In the nematic phase of **C_6O** the error of ε is greater than in the smectic phases.

The different tilt angles of the two legs must be implied by the ester-groups connecting ring C with the legs. Their shift anisotropies are quite different ($\delta_{\zeta\zeta}^{COO}=43$ ppm, $\delta_{\zeta\zeta}^{COO'}=7$ ppm). The low value can only be explained by a nonplanar ester group with a torsion about the bond from ring C to O(CO). This rotation changes the direction of the following rings.[5,10] So the small tilt on the same site as the CN group can be understood similar as for the Cl-substituted molecules.[5] Both $\delta_{\zeta\zeta}^{COO}$ change their values at the SmA–SmC transition in **C_6O** and the SmC–B_2 transition in **C_{14}**, indicating a connection between the shifts and the geometry of the legs.

Fig. 9 gives the bending-angle ($180°-\varepsilon_A-\varepsilon_{A'}$) of the two molecules as a function of temperature. For **C_6O** the bend increases within the SmA phase and particularly after the transition into the SmC phase. The **C_{14}** molecules have nearly the same bending angle, but here a jump to stronger bend occurs only at the transition to the B_2 phase.

The behaviour of the aliphatic chains is only observable for **C_6O**. Besides the small anisotropies a different geometry of the two chains is detected until the last segment x6. The averaged conformation is distinguishable. Typically for chains is the increase of $\delta_{\zeta\zeta}^{xn}$ with decreasing temperature, but here the anisotropy of the first methylene groups in both legs decreases which is an indication of torsion of this group around the *para*-axis.

X-Ray investigations

Fig. 10a–c displays the patterns of oriented samples in the SmA, SmC and B_2 phases of compound **C_6O**. The pattern in the SmA phase (Fig. 10a) exhibits the same specific feature as known in the case of rod-like molecules: the spot-like layer reflections are positioned at the meridian of the pattern and the outer diffuse scattering is located around the equator. It can be

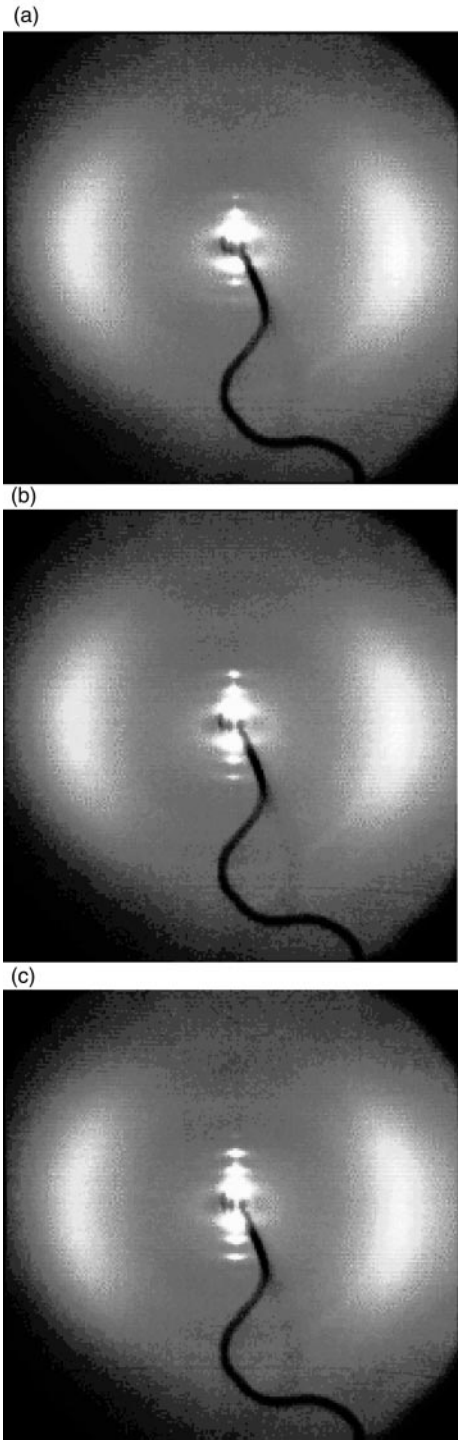

Fig. 10 X-Ray patterns of monodomains: a) of the SmA phase (145 °C), b) the SmC phase (120 °C), c) the B_2 phase (80 °C) of compound **C_6O**.

understood only if the banana-shaped molecules are rotational disordered around an averaged molecular axis. Thereby, the pattern is comparable with those of parallel oriented rods.

Cooling down the sample from the SmA phase into the SmC phase and further into the B_2 phase an essential alteration of the pattern can not be seen (Fig. 10b and c). In the B_2 and SmC phase the profile of the outer diffuse scattering as a function of χ is more flattened (χ is measured from the equator) (Fig. 11). An analysis of the profile leads to two maxima shifted by an angle of 29° (Fig. 12). That proves the existence of a small tilt angle α of about 14–15° in agreement with electro-optical measurements.

The layer spacings are nearly independent of the temperature

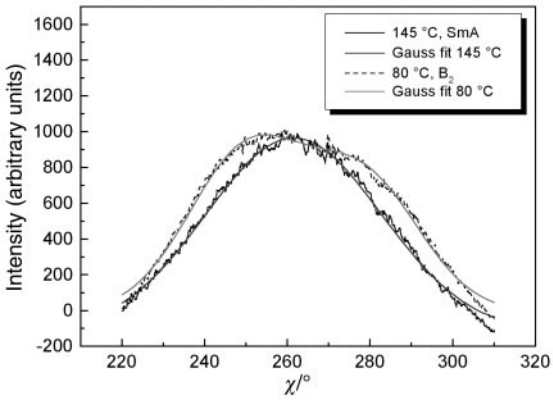

Fig. 11 χ-Scans on the X-ray patterns in the SmA phase and the B_2 phase of compound $\mathbf{C_6O}$.

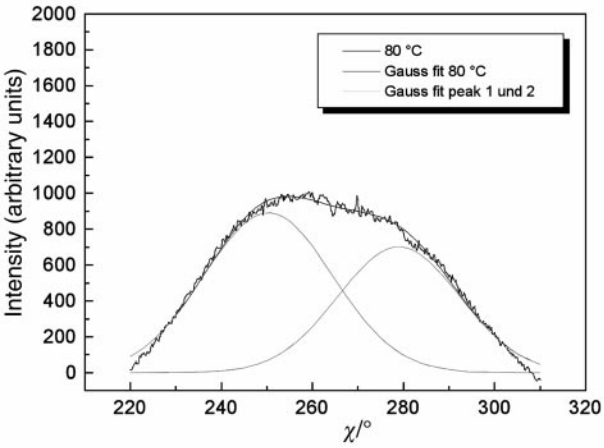

Fig. 12 Detailed analysis of the χ-scan in the B_2 phase of compound $\mathbf{C_6O}$. The profile has been fitted by two Gaussian functions whereby the two maxima correspond to the χ-angles 250° and 279°. The difference between the two maxima is twice of the tilt angle.

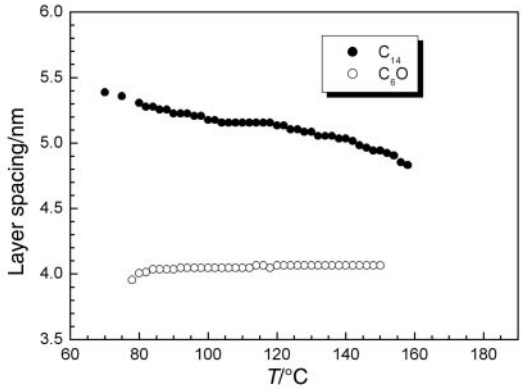

Fig. 13 Temperature dependence of the layer spacings in the SmA, SmC and B_2 phases of compounds $\mathbf{C_6O}$ and $\mathbf{C_{14}}$, respectively.

in the case of the hexyloxy compound. A more detailed investigation of higher homologues provides the unusual result that the *d*-values increase continuously with decreasing temperature in the SmA phase as well as in the SmC phase. Fig. 13 displays the two extreme cases ($\mathbf{C_6O}$, $\mathbf{C_{14}}$).

Usually the *d*-values decrease in the SmC phase because of the inclination of the molecules. In this case the tilt angle α of the molecules in the SmC phase can be estimated *via* $\cos\alpha = d_C/d_A$, where d_C and d_A are the layer spacings in the SmA and SmC phase, respectively. This estimation is based on the assumption that the conformation and the order parameter *S* are the same in both phases. As shown in the preceding section *S* strongly increases with decreasing temperature and is essentially higher in the SmC phase and B_2 phase. The increase of *S* as well as the possible change of the chain conformation (decrease of *gauche* conformations with decreasing temperature) can explain the unusual increase of the layer thickness with decreasing temperature in the case of the higher homologues although a SmC phase with a tilted structure is experimentally proved. In the case of compound $\mathbf{C_6O}$ a change of a chain conformation can not be expected. On the other hand, the NMR measurements prove a decreasing bending angle with falling temperature which would lead together with a tilt angle to a lowering of the *d*-values. The increasing order parameter, however, has the opposite effect. In this way the nearly temperature-independent layer spacing in the mesophase of compound $\mathbf{C_6O}$ can be understood as a result of two counteracting factors.

It could be possible that the biaxial smectic phase between the SmA and B_2 phase is a biaxial SmA phase (SmA_b) which was discussed by Brand *et al.*[14] and which has recently been investigated experimentally by Prathiba *et al.*[15] and Hegmann *et al.*[16] But the existence of such a phase can be ruled out for different reasons. The *schlieren* texture of this phase does not show disclinations of half-integer strength; furthermore this phase exhibits a broken fan-shaped texture. Both findings are incompatible with a SmA_b phase. Also the occurence of the electrohydrodynamic pattern as found for compound $\mathbf{C_9O}$ is characteristic for a SmC phase.

Above all, the maxima of the diffuse scattering in the wide angle region were found out of the equator which is not compatible with a SmA_b phase but with a tilted smectic phase.

Discussion

The bent molecular shape is obviously a necessary precondition for the formation of the new phases which are designated by the code letters B_1–B_7. It follows from previous NMR investigations that the bending angle in the liquid-crystalline state (the angle between the two legs of the banana-shaped molecules) varies between 105° and 140° depending on the chemical structure of the molecules. If this angle is smaller or greater than these limits typical mesophases of calamitic compounds occur such as nematic, SmA or SmC phases. It seems that in the case of the studied cyano-substituted banana-shaped compounds the bending angle is just at one of the limits ($\sim$140°) which would explain the simultaneous occurence of the B_2 phase (typical for a bent molecular shape) and SmA and SmC phases (typical for calamitic molecules). We can assume that the bent molecules can freely rotate in the SmA phase giving rise to the uniaxial structure. In the SmC phase the molecules are weakly tilted, but according to dielectric investigations ferroelectric clusters in the short range arise. On further cooling the long-range packing of the molecules in the bent direction becomes more favourable for steric reasons, but the tilt of the molecules is preserved. The alternating polar direction in subsequent layers causes the antiferroelectric character of the ground state and stabilizes the layer structure of the B_2 phase by minimizing of the Coulomb energy.

Experimental

The phase transition temperatures were determined by differential scanning calorimetry (DSC 7, Perkin Elmer) and by polarizing microscopy (Leitz Orthoplan, equipped with a Linkam THM 600/S hot stage). An initial identification of the mesophases was carried out on the basis of their optical texture. X-Ray diffraction measurements on non-oriented samples were performed with a focusing Guinier goniometer and a Guinier

film camera (Huber Diffraktionstechnik GmbH) or small angle equipment. The samples were filled in glass capillaries (id 1 mm), the temperature was controlled better than ±1 K. X-Ray measurements on oriented samples were carried out with a 2D detector (HI-Star, Siemens AG). The alignment of the samples was achieved by annealing a drop of the liquid crystal on a glass plate immediately below the clearing temperature. In the case of compound **C_6O** the homogeneous orientation was obtained in the nematic state by applying a magnetic field (0.7 T). Electro-optical measurements were made using the usual experimental set-up described in an earlier paper.[5] The spontaneous polarization was measured with the triangular wave voltage method using the same set-up.

NMR measurements were performed with a Bruker MSL 500 spectrometer at a magnetic field of 11.7 T. The samples were put in standard 5 mm tubes. The proton decoupled ^{13}C spectra at 125 MHz, without spinning, are well resolved in the isotropic liquid. We used pulse and CP excitation for ^{13}C resonance and observed the spectra using continuous and pulsed decoupling (Waltz). In the case of continuous irradiation the decoupling efficiency in the different regions of the spectra depends on the proton frequency offset.

The director orientation of the samples in the smectic A and C phases are perfect, giving sharp spectral lines. In the nematic phase the line widths are greater.

Synthetic procedure

The structure of the products was proved by ^1H NMR spectroscopy (Varian Gemini 200 and Varian Unity 400), mass spectroscopy (Intectra GmbH, AMD 402, electron impact, 70 eV); Finnigan MAT LCQ Spectrometer and IR spectrometer Bruker IFS 66. Elemental analysis were performed using a CHNS-932 (Leco Co.) elemental analyser.

2,4-Dihydroxybenzonitrile. A solution of 2,4-dihydroxybenzaldehyde (22.5 g, 0.16 mol) in 60 ml of ethanol was treated with a concentrated aqueous solution of hydroxylamine hydrochloride (16.7 g, 0.24 mol) followed by slow addition of a concentrated aqueous solution of $Na_2CO_3{\cdot}10H_2O$ (22.9 g, 0.08 mol). Crystals were obtained and isolated by filtration. Recrystallisation from water gives 22.3 g (91%) of the 2,4-dihydroxybenzaldoxime. Mp 190–192 °C (ref. 8 191 °C). The solid was then dissolved and refluxed in 90 ml of acetic anhydride for 3 h. The solvent was removed *in vacuo*. The product was recrystallized from ethanol to give 14 g (44%) of the acetylated intermediate. This product (0.064 mol) was treated with aqueous KOH solution (12 g of KOH in 55 ml of water), and the resulting solution was stirred for 3 days at ambient temperature. Careful acidification (pH 2) with dilute sulfuric acid (20 vol%) was followed by extraction with ethyl acetate (3 × 50 ml). The pooled organic phases were dried over Na_2SO_4, and the solvent was removed *in vacuo*. The product was purified by column chromatography on silica gel using ethyl acetate–heptane (20 : 1) as eluent. Yield 7 g (82%). Mp 174–175.5 °C (Mp 175 °C[8]). ^1H NMR (200 MHz DMSO-d_6) δ: 10.03 (s, 2H, OH), 6.56–6.50 (m, 3H, Ar). IR (Nujol) $\nu_{CN} = 2230\ cm^{-1}$.

4-Cyano-1,3-phenylene bis[4-(4-*n*-alkyl- or -alkoxy-phenyliminomethyl)benzoates] C_{12}, C_{14}, C_6O, C_8O, C_9O, $C_{12}O$. The mixture of 0.18 g (1.3 mmol) of 2,4-dihydroxybenzonitrile, 2.6 mmol of the corresponding 4-(4-alkyl- or -alkoxy-phenyliminomethyl)benzoic acid,[10] 0.56 g (2.7 mmol) DCC, and DMAP as catalyst in 40 ml of dichloromethane was stirred at room temperature for 24 h. The precipitate was filtered out, the solvent was evaporated. The products were recrystallised from DMF–ethanol.

C_8O (R = $C_8H_{17}O$). ^1H NMR (400 MHz, $CDCl_3$) δ: 0.87 (t, ^3J = 6.8 Hz, 6H, CH_3), 1.28–1.49 (m, 20H, CH_2), 1.75–1.82 (m, 4H, OCH_2CH_2), 3.97 (t, ^3J = 6.5 Hz, 4H, OCH_2), 6.93 (dd, ^3J = 9.0 Hz, ^4J = 2.7 Hz, 4H, Ar), 7.28 (dd, ^3J = 8.8 Hz, ^4J = 1.6 Hz, 4H, Ar), 7.33 (dd, ^3J = 8.5 Hz, ^4J = 2.2 Hz, 1H, Ar), 7.56 (d, ^4J = 2.2 Hz, 1H, Ar), 7.80 (d, ^3J = 8.4 Hz, 1H, Ar), 8.03 (d, ^3J = 8.4 Hz, 4H, Ar), 8.25 (d, ^3J = 8,4 Hz, 2H, Ar), 8.32 (d, ^3J = 8.4 Hz, 2H, Ar), 8.57 (s, 2H, CH=N). Elemental analysis for $C_{51}H_{55}N_3O_6$ (805.95): calcd: C 76.00, H 6.88, N 5.21; found: C 75.76, H 6.57, N 4.83. IR (KBr) ν_{CN} 2227cm^{-1}. MS *m*/*z* (rel intensity): 806 (10), 805 (47), 556 (18), 470 (15), 336(100), 241 (42), 224 (43), 195 (41), 69 (21).

C_{12} (R = $C_{12}H_{25}$). ^1H NMR (200 MHz $CDCl_3$) δ: 0.88 (t, ^3J = 6.2 Hz, CH_3), 1.27–1.51 (m, 36H, CH_2), 1.62–1.78 (m, 4H, Ar-CH_2CH_2), 2.64 (t, ^3J = 7.6 Hz, 4H, Ar-CH_2), 7.26 (s, 8H, Ar), 7.36 (dd, ^3J = 8.7 Hz, ^4J = 2.2 Hz, 1H, Ar), 7.59 (d, ^4J = 2.0 Hz, 1H, Ar), 7.82 (d, ^3J = 8.8 Hz, 1H, Ar), 8.07 (d, ^3J = 7.4 Hz; ^4J = 1.6 Hz, 4H, Ar), 8.27–8.37 (m, 4H, Ar), 8.59 (s, 2H, CH=N).

C_{14} (R = $C_{14}H_{29}$). ^1H NMR (200 MHz $CDCl_3$) δ: 0,88 (t, ^3J = 6.3 Hz, 6H, CH_3), 1.27–1.52 (m, 44H, CH_2), 1.59–1.72 (m, 4H, Ar-CH_2CH_2), 2.64 (t, ^3J = 7.6 Hz, 4H, Ar-CH_2), 7.25 (s, 8H, Ar), 7.36 (dd, ^3J = 8.6 Hz, ^4J = 2.2 Hz, 1H, Ar), 7.59 (d, ^4J = 2.2 Hz, 1H, Ar), 7.83 (d, ^3J = 8.7 Hz, 1H, Ar), 8.07 (dd, ^3J = 6.6 Hz; ^4J = 1.6 Hz, 4H, Ar), 8.26–8.37 (m, 4H, Ar), 8.59 (s, 2H, CH=N).

C_6O (R = $C_6H_{13}O$). ^1H NMR (200 MHz $CDCl_3$) δ: 0.90 (t, ^3J = 6.5 Hz, 6H, CH_3), 1.23–1.50 (m, 12H, CH_2), 1.72–1.82 (m, 4H, OCH_2CH_2), 3.98 (t, ^3J = 6.6 Hz, 4H, OCH_2), 6.93 (d, ^3J = 8.8 Hz, 4H, Ar), 7.28 (d, ^3J = 8.8 Hz, 4H, Ar), 7.35 (dd, ^3J = 8.6 Hz, ^4J = 2.1 Hz, 1H, Ar), 7.56 (d, ^4J = 2.0 Hz, 1H, Ar), 7.80 (d, ^3J = 8.6 Hz, 1H, Ar), 8.03 (d, ^3J = 8.5 Hz, 4H, Ar), 8.23–8.34 (m, 4H, Ar), 8.57 (s, 2H, CH=N).

C_9O (R = $C_9H_{19}O$). ^1H NMR (400 MHz $CDCl_3$) δ: 0.87 (t, ^3J = 6.8 Hz, 6H, CH_3), 1.28–1.49 (m, 12H, CH_2), 1.71–1.82 (m, 4H, OCH_2CH_2), 3.97 (t, ^3J = 6.6 Hz, 4H, OCH_2), 6.93 (d, ^3J = 8.9 Hz, ^4J = 2.7 Hz, 4H, Ar), 7.28 (d, ^3J = 8.9 Hz, 4H, Ar), 7.33 (dd, ^3J = 8.6 Hz, ^4J = 2.1 Hz, 1H, Ar), 7.56 (d, ^4J = 2.1 Hz, 1H, Ar), 7.80 (d, ^3J = 8.6 Hz, 1H, Ar), 8.03 (dd, ^3J = 8.4 Hz, ^4J = 2.0 Hz, 4H, Ar), 8.24–8.33 (m, 4H, Ar), 8.57 (s, 2H, CH=N).

$C_{12}O$ (R = $C_{12}H_{25}O$). ^1H NMR (200 MHz $CDCl_3$) δ: 0.86 (t, ^3J = 6.4 Hz, 6H,CH_3), 1.25–1.44 (m, 20H, CH_2), 1.72–1.82 (m, 4H, OCH_2CH_2), 3.97 (t, ^3J = 6.6 Hz, 4H, OCH_2), 6.93 (d, ^3J = 8.8 Hz, 4H, Ar), 7.28 (d, ^3J = 8.8 Hz, 4H, Ar), 7.34 (dd, ^3J = 8.8 Hz, ^4J = 2.2 Hz, 1H, Ar), 7.56 (d, ^4J = 2.2 Hz, 1H, Ar), 7.80 (d, ^3J = 8.6 Hz, 1H, Ar), 8.03 (dd, ^3J = 8.3 Hz, ^4J = 2.0 Hz, 4H, Ar), 8.23–8.34 (m, 4H, Ar), 8.57 (s, 2H, CH=N).

Acknowledgements

This work was supported by the Deutsche Forschungsgemeinschaft (DFG) and the Fonds der Chemischen Industrie.

References

1 T. Niori, T. Sekine, J. Watanabe, T. Furukawa and H. Takezoe, *J. Mater. Chem.*, 1996, **6**, 1231.
2 W. Weissflog, Ch. Lischka, I. Benne, T. Scharf, G. Pelzl, S. Diele and H. Kruth, *Proc. SPIE – Int. Soc. Opt. Eng.*, 1998, **3319**, 14.
3 A. Jakli, S. Rauch, D. Lötzsch and G. Heppke, *Phys. Rev. E*, 1998, **57**, 6737.
4 D. R. Link, G. Natale, R. Shao, J. E. Maclennan, N. A. Clark, E. Körblova and D. M. Walba, *Science*, 1997, **278**, 1924.
5 G. Pelzl, S. Diele, S. Grande, A. Jakli, Ch. Lischka, H. Kresse,

H. Schmalfuss, I. Wirth and W. Weissflog, *Liq. Cryst.*, 1999, **26**, 401.
6 G. Pelzl, S. Diele and W. Weissflog, *Adv. Mater.*, 1999, **11**, 707.
7 W. Weissflog, L. Kovalenko, I. Wirth, S. Diele, G. Pelzl, H. Schmalfuss and H. Kresse, *Liq. Cryst.*, 2000, **27**, 677.
8 J. L. Serrano, T. Sierra, Y. Gonzalez, C. Bolm, K. Weickardt, A. Magnus and G. Moll, *J. Am. Chem. Soc.*, 1995, **117**, 8312.
9 E. Marcus, *Chem. Ber.*, 1891, **24**, 3650.
10 W. Weissflog, Ch. Lischka, S. Diele, G. Pelzl, I. Wirth, S. Grande, H. Kresse, H. Schmalfuss, H. Hartung and A. Stettler, *Mol. Cryst. Liq. Cryst.*, 1999, **333**, 203.
11 M. Petrov and G. Durand, *J. Phys. Lett.*, 1981, **42**, L-519.
12 S. Diele, S. Grande, H. Kruth, Ch. Lischka, G. Pelzl, W. Weissflog and I. Wirth, *Ferroelectrics*, 1998, **212**, 169.
13 T. M. Ducan, *A Compilation of Chemical Shift Anisotropies*, Farragut Press, Chicago, 1990
14 H. R. Brand, P. E. Cladis and H. Pleiner, *Macromolecules*, 1992, **25**, 7223.
15 R. Prathiba, N. V. Madhusudana and B. K. Sadashiva, *Science*, 2000, **288**, 2184.
16 T. Hegmann, J. Kain, S. Diele, G. Pelzl and C. Tschierske, *Angew. Chem., Int. Ed.*, 2001, **40**, 887.